Rock Mechanics for Natural Resources and Infrastructure Development – Fontoura, Rocca & Pavón Mendoza (Eds)

Amount of fracturing inside rock slopes due to strength variation

A.K. Alzo'ubi
Abu Dhabi University, Al Ain, Abu Dhabi, United Arab Emirates

ABSTRACT: In rock slopes prone to topple, mechanical, physical, and/or chemical weathering might degrade the rock mass properties and compromise the stability of that rock slope. This paper investigates the effect of tensile strength degradation on the fracturing amount inside two rock slopes prone to topple. The first example is an ideal slope with one indipping joint set and the second one is an open pit mine from Canada. The simulation in this paper uses a discrete element model with Voronoi tessellation joint pattern to examine fracturing inside the rock mass due to the reduction of tensile strength, which simulates a weathering process. For the ideal slope, the fracturing amount was measured along the most possible rupture surface at different tensile strength values. While, the fracturing amount inside the open pit slopes was also traced along three different paths located near the most possible rupture surfaces as observed numerically. This study uses the ratio between the total length of fractures along or crossing a selected path and the entire length of the path itself and its called "Percent Fracturing". The tensile strength of the rock mass was changed to show the effect of this variation the percent of fracturing. As show in the numerical model, amount of fracturing decreased as the tensile strength increased. This parametric study showed that the amount of fracturing rock slopes susceptible to toppling is highly influenced by the tensile strength values. The effect of friction and cohesion of intact material were not discussed in this paper.

1 INTRODUCTION

Rock slopes can move in different styles such as; toppling, falling, and sliding; depending on the rock mass characteristics, joints orientation and other factors as discussed by Alzo'ubi, 2016. This paper presents two rock slopes susceptible to toppling movement to study the effect of tensile strength on the fracturing amount inside rock slopes. Toppling has been under analysis since the 1970's when De Freitas and Watters, 1973, introduced the term "toppling". Later, Goodman and Bray, 1976, discussed toppling and classified this type of movement into three different styles, block toppling, flexural, and block-flexural toppling. This paper discusses the amount of fracturing inside rock slopes suffered from toppling movement due to tensile strength reduction to show the importance of this strength parameter.

In geology, Terzaghi, 1962, discussed two types of joint orientations in two types of rocks. He stated that in sedimentary rocks, the beddings are perpendicular to the cross-joints and the thickness of the beds ranges from centimeters to meters in sedimentary rocks. However, in crystalline rocks, he described a geological model with irregular-shaped crystalline blocks in which the jointing is a random and the cross-joints are usually not perpendicular to the main set of joints. Nichol et al., 2002, studied such slopes where the secondary joint set is not perpendicular to the in-dipping set. The first example in this paper uses a very similar slope to the one used by Nichole et al., 2002 to examine fracturing inside the rock slope.

Moreover, Tosney, 2001, investigated the toppling in an open pit mine where two sets of joints exist, the thickness of the rock columns in plutonic rocks in this open pit mine can be as much as 40 meters. The mine is located in British Columbia 75 km southwest of Kamloops and consisted of two pits; the Lornex Pit and the Valley Pit, the second numerical model in this paper simulates the Lornex pit.

The two above mentioned slopes; the ideal one and the southeast wall of the Highland Valley Copper (HVC) were simulated by using the UDEC-DM (Alzo'ubi et. al., 2007). This numerical method provides tools to investigate fracturing amount inside rock masses. This study uses the ration between the total lengths of the fracture joints, crosses the most possible rupture surface path, and the length of that path to study the tensile strength degradation effect due to weathering on this ration.

2 IDEAL ROCK SLOPE

In this example, an ideal rock slope with one set of in-dipping joints is simulated by utilizing the UDEC-DM (Alzo'ubi et al. 2007). The Voronoi tessellation joint pattern was used to generate randomly shaped blocks. The rock slope has a height of 350 m as shown in Figure 1, the main set of joints formed approximately 80° angle with the horizontal. Table 1 presents the material properties for this numerical model. The Coulomb-slip model was used to control the flaws' behavior, and the blocks formed by the flaws were assumed to behave in an elastic fashion with an E = 20 GPa and a ν = 0.25.

The inset in Figure 1 shows the Voronoi flaws, these flaws properties simulate the intact material properties as shown in the Table above. At first, the flaws in this model were assigned a 1 MPa of tensile strength and the other properties mentioned in Table 1, at this tensile strength a continuous failure surface formed inside the slope as shown in Figure 2. To examine the tensile strength effect, I increased the tensile strength to 6.9 MPa until equilibrium reached. At that point, the measured fracturing percentage, of the joints crossing the most probable rupture surface, was 50%. These preliminary results indicated that tensile strength could limit the fracturing amount inside a rock slope prone to topple, in the next a large open pit mine is analyzed to verify these preliminary results.

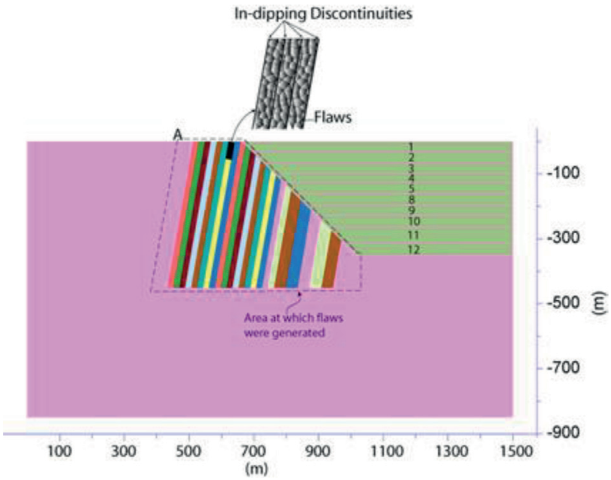

Figure 1. The ideal rock slope model.

Table 1. Toppling slope numerical simulation properties.

Properties	Flaws	In-dipping joints
Φ°	30	30
Cohesion (MPa)	5.0	5.0
Kn (GPa/m)	40	10
Ks (GPa/m)	20	1
Tensile Strength MPa	1	0.0

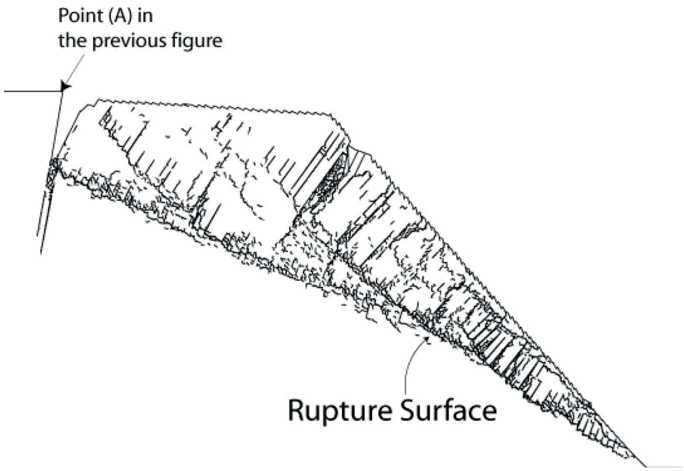

Figure 2. Rupture surfaces formation.

3 OPEN PIT MINE

The geological analysis of the Pit under investigation revealed two major sets of discontinuities. The first set of joints is persistent and dips into the slopes at angles between 70° and 80° with a spacing between 20 and 40 m. The second set is non-persistent and dips in the same direction as the slope face at angles ranging between 50° and 60° from the horizontal with an average spacing between 10 m and 20 m.

The mine engineers used the RMR classification system (Bieniawski, 1976) to estimate the strength properties of the different geological units encountered at the pit. The results of the mapping are presented in Figure 3. Moreover, Tosney, 2001 used Hoek and Brown, 1988, failure criterion to estimate the Mohr-Coulomb strength parameters necessary to conduct stability analysis for this slope. Table 2 summarizes the properties used in this paper. Tosney, 2001, and the site engineers estimated the tensile strength at 0.1 MPa for all the geological units, which is at the low end of the tensile strength range for the material forming this slope.

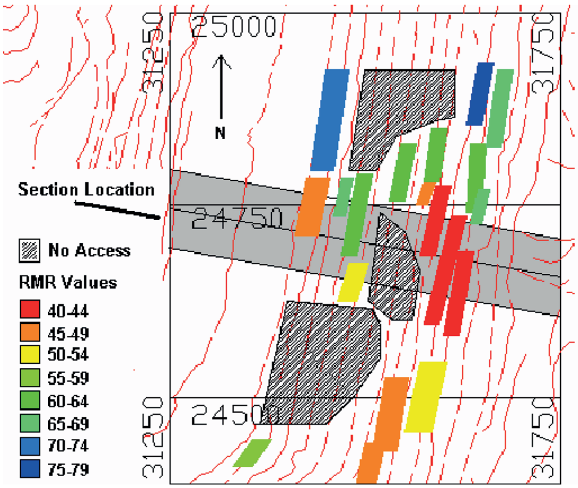

Figure 3. The RMR rating of the pit (modified from Tosney et al., 2004).

Table 2. Mohr-Coulomb properties used in the numerical model.

RMR 76	φ(°)	C (MPa)	E (GPa)	G (GPa)	K (GPa)
40	29	0.7	5.6	2.2	4.7
60	43	1.0	17.8	6.8	14.8
80	54	2.1	56.2	21.6	46.9

Table 3. The discontinuities properties used in the model, Alzo'ubi et al., 2012.

Parameter	In Dipping faults	Secondary discontinuities
Orientation (°)	70	125
Normal Stiffness (GPa/m)	4	4
Shear Stiffness (GPa/m)	1	1
Cohesion (kPa)	6.0	0
Friction (°)	12	25

The numerical simulation in this study incorporated the two sets of joints as persistent joints, Table 3 shows the properties of these two sets.

3.1 *Displacement monitoring and movement*

To monitor the displacement magnitude and rate, the engineers installed slope-monitoring prisms. Newcomen et al., 2003b, described the monitoring system used in the pit to record the slope surface movement. I used these displacements to calibrate the model and to compare the numerical model results with the actual ones observed in the field to form a baseline for comparison purposes.

3.2 *The numerical model and calibration*

Alzo'ubi et al., 2007, introduced the UDEC-DM method, this approach can simulate fracturing of intact rock material whenever, the stress exceeds the strength of the material. This section uses the southeast wall of the Lornex pit to investigate the effect of tensile strength amount of fracturing inside the rock slope.

Alzo'ubi et al., 2012, discussed the geometry of the model based on the actual mining steps of this mine, Figure 4. The two sets of joints were modeled explicitly; the in-dipping joints with an angle of 70° and spaced at 30 m, while the out-dipping joints at an angle of 55° from the horizontal

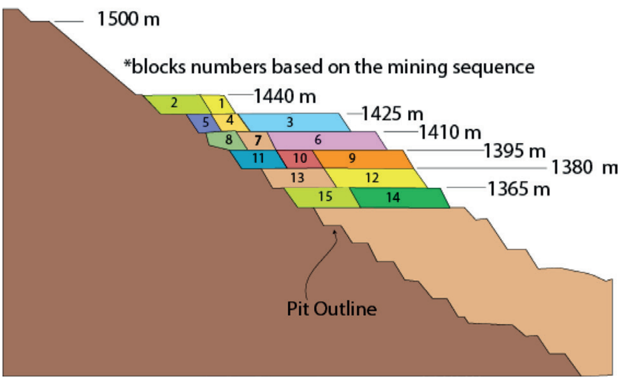

Figure 4. Blocks excavation sequence at Lornex southeast wall (from Alzo'ubi, 2009).

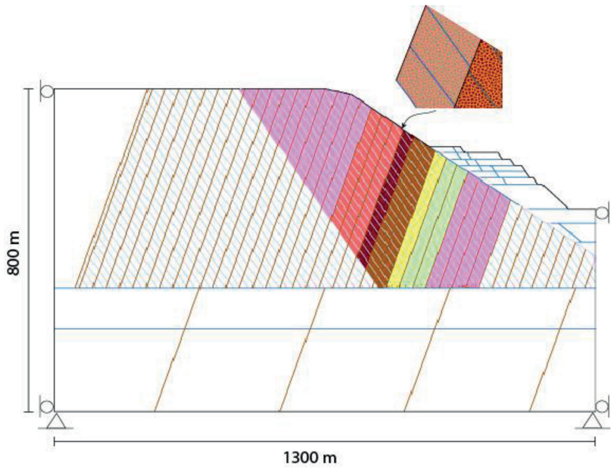

Figure 5. The southeast wall UDEC-DM; the inset shows the details of the generated flaws.

and spaced at 15 m. The two intersecting joints form blocks, and each block was dissected by the Voronoi joints pattern with a 1.4 m edge length. This process generated randomly polygonal blocks as shown in the inset of Figure 5.

In this model and during the mining of blocks 1 to 15, four slope-monitoring prisms were utilized to track the mining-induced deformation along this section. The modeling process started by bringing the model to equilibrium under high strength properties and then the model was calibrated to avoid the unrealistic numerical behavior at the initial stage and then properties that are more realistic were assigned to the model. The deformation at the location of by SMP number 413 (Alzo'ubi et al. 2012) was used to calibrate the model at two mining steps.

The normal and shear stiffnesses that were used in this model are shown in Table 4, at these values a good agreement between the calculated and observed displacement was achieved.

3.3 *The numerical model results*

After the model reached equilibrium, the actual strength properties presented in the above sections were used. The modeling process started by simulating the excavation of blocks 1 to 15, one block at a time. After excavating each block, the model continued to run until equilibrium reached. For each run, the fracturing throughout the model was monitored to compare the numerical behavior with the field observations.

To investigate the slope behavior under variation of the tensile strength parameter, the amount of fracturing in the slope due to the variation of the tensile strength parameter was measured along path number 1, which is situated along the most possible rupture surface as observed in the numerical simulation, Figure 6.

The fractured joints along the selected paths were mapped, measured, and normalized to the entire length of the path to calculate the percentage of fracturing. Initially, 25.1 % of the entire

Table 4. Normal and shear stiffness resulting from the calibration process

RMR 76	Normal Stiffness (GPa/m)	Shear Stiffness (GPa/m)
40-44	11	3.5
45-49	14	4.5
60-64	34	11

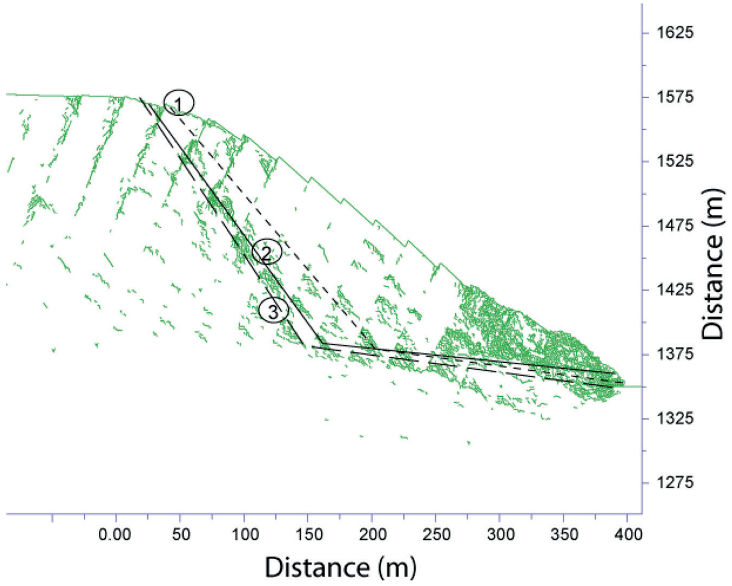

Figure 6. The paths used to trace the percentage of fracturing in the numerical model

length of the path fractured in the model as shown in Figure 6. To see this effect of tensile strength on fracturing, I used another four values of tensile strength 0.1, 0.2, 0.4, 0.7, and 1 MPa and calculated the percentage of fracturing along the same path. The results show that the maximum tensile strength of the material decreased the percent of fracturing to less than 10%. Alzo'ubi, 2018, showed that transitory stresses might also cause similar fracturing at the same tensile strength. Figure 7 shows that the fracturing percentage decreased as the tensile strength increased. It is clear that tensile strength has a major part in controlling the amount of fracturing in the rock slope as discussed in this paper. The percent of fracturing at 1.0 MPa decreased to 7% which is far less than the model at the 0.1 MPa tensile strength model. Figure 8 shows the model, at 1.0 MPa tensile strength, after excavating block number 15 and reaching equilibrium. Notice the visual differences in the fracturing amount between Figure 6 and 8.

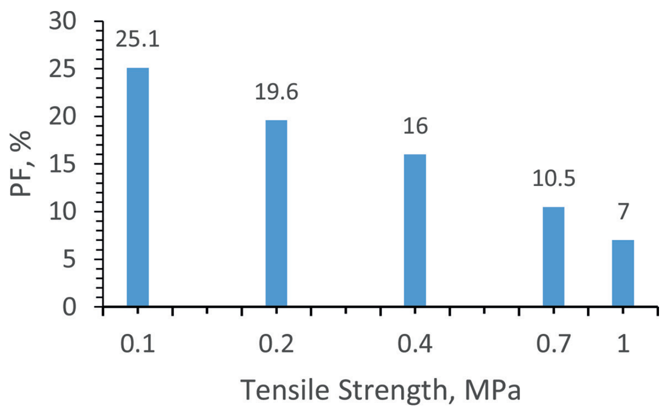

Figure 7. Percent fracturing (%) with tensile strength variation.